Combinatorial Considerations on a Two-Dimensional Toy Model for Quantum Gravity

Bachelor Thesis

Daan Janssen
Supervised by Professor Renate Loll

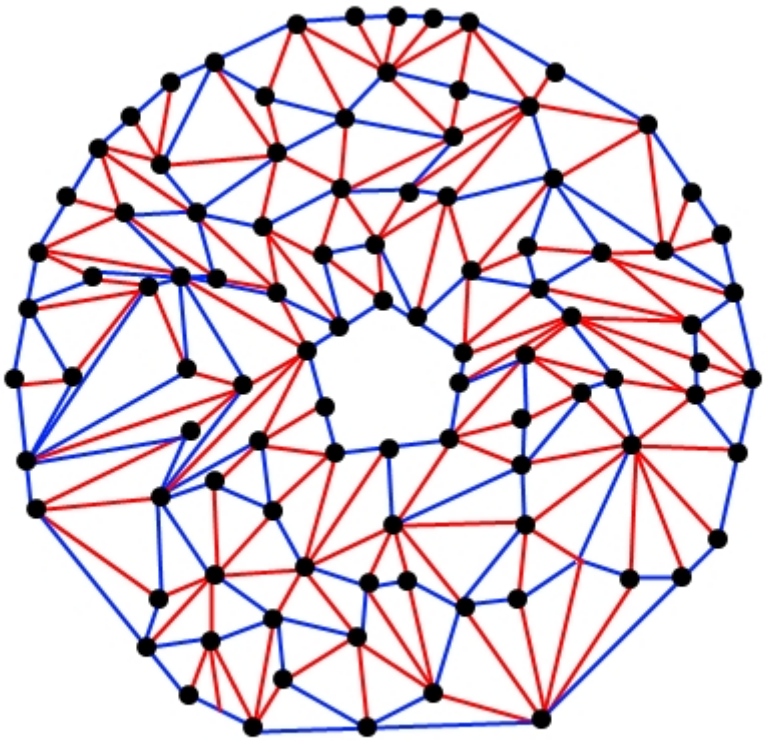

Contents

1 Introduction

This thesis is the result of a bachelor intern-ship that is part of a double bachelor degree in Physics & Astronomy and Mathematics at the Radboud University Nijmegen. Part of this research internship has also been done as in association with the Radboud Honours Programme FNWI. For this project I was supervised by Professor Renate Loll from the Institute of Mathematics, Astrophysics and Particle Physics at Radboud University. The main topic of this thesis is an analytical study of a discrete toy model for Quantum Gravity in two dimensions, where the goal is to find a continuum limit of this model. This model, known as Locally Causal Dynamical Triangulations, is a generalization of the Causal Dynamical Triangulations model, of which the two dimensional case has been completely solved.

The 20th century has been one of the most revolutionary ages for physics in history. Two great insights have changed the way we view the universe forever. The discovery of the theory of General Relativity (GR), which can be largely attributed to Albert Einstein, has revealed the relation between gravity and the geometry of space-time. Secondly, in discovering the theory of Quantum Mechanics (QM), we have learned the intricate mechanisms that govern nature on very small scales. Usually these two theories don't have to be considered at the same time to study physical phenomena. As GR is associated with large scale astrophysical or even cosmological phenomena, while QM mostly plays an important role at molecular scales or smaller (depending on the interactions involved), there are only a few cases where these two theories have to meet. In most of these cases it is sufficient to consider QM on some fixed GR background, when gravitational effects become strong enough to have a relevant influence on the QM system. A famous example of this is Hawking radiation [1], which is concerned with pair creation of a particle and its antiparticle on the GR background of a black hole event horizon. In these kinds of phenomena, one only takes into account the quantum nature of particles and fields that live in space-time, however, they do not take into account the quantum nature of space-time itself.

As of today, we understand the quantum origin of the three of the four fundamental forces and the particles involved quite well. We have been able find a quantum theory of electromagnetism, the weak interaction and the strong interaction. Even though there are still a lot of open questions about these forces and particles, these question fade in comparison to the gap in our knowledge about the fourth fundamental force, gravity. So far no-one has been able to write down a consistent and complete quantum theory of gravity. This makes the field of Quantum Gravity (QG), as the study of the quantum nature of gravity and space-time is called, a highly active field of research in which theorists from all over the world work to develop such a quantum theory.

The scale at which we expect quantum phenomena of gravity and space-time to start playing a role, is known as the Planck length. This length scale can be found by a dimensional analysis of the constants of nature involved in the theory of QM, Plancks constant $\hbar$, and in GR, the speed of light c and Newton's constant G_N. From this one finds the Planck length to be [2]

$$\ell_P = \sqrt{\frac{G_N \hbar}{c^3}} = 1.6 \times 10^{-35} \text{ m}. \tag{1}$$

This is a very short length which at this point we cannot probe directly by experiments, which makes QG a largely theoretical subject. Nevertheless we expect QG to be of vital importance for our understanding of singularities in space-time, which are predicted by classical GR at the center of black holes or at the beginning of our universe (the Big Bang). After all, singularities are points in space-time and are therefore much "smaller" than the Planck length.

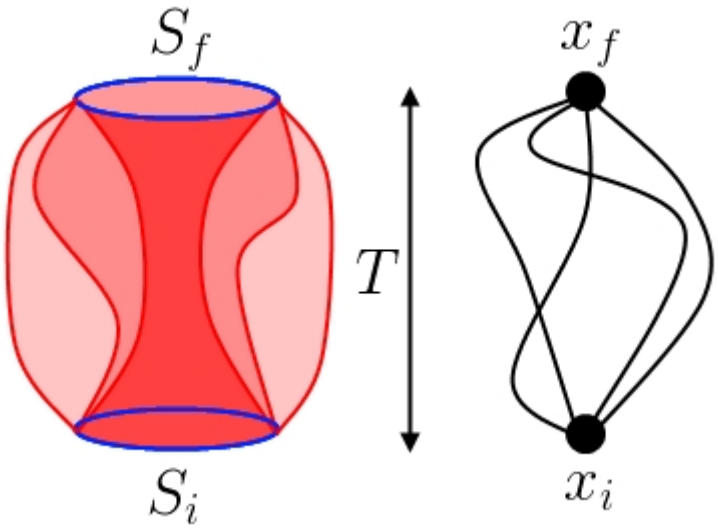

Figure 1: Space-times connecting two spatial geometries (left) and paths connecting two points in space-time (right)

2 A Path Integral approach to Quantum Gravity

As a starting point for a theory of Quantum Gravity, we try to combine aspects from both QM and GR into a single formalism. In our case we let ourselves be inspired by the path integral formalism of QM. Here we imagine a particle measured at some point x_i in space and leave the system to evolve, then after some time T we wish to know where we can measure the particle by then. To do that we can try to find some (complex valued) transition amplitude $G(x_i, x_f; T)$ (we call this function a propagator), from which we can calculate the probability of now finding a particle at position x_f. This propagator is given by a path integral, where each possible path $\mathbf{q}$ from x_i at time 0 to x_f at time T gets assigned a value, where-after we sum/integrate over the space of all paths,

$$G(x_i, x_f; T) = \int_{\mathbf{q}(0)=\mathbf{x}_i}^{\mathbf{q}(T)=\mathbf{x}_f} D\mathbf{q} \exp\left(iS(\mathbf{q})\right). \tag{2}$$

The value assigned to each path $\mathbf{q}$ is given by the complex value $\exp\left(iS(\mathbf{q})\right)$, where $S(\mathbf{q}) = \int_0^T dt \frac{m}{2}\dot{\mathbf{q}}(t)^2 - V(\mathbf{q}(t))$ is the classical action for a path of mass m in a potential V. Note that the integral over a function space is not clearly defined, in this case one can define this expression as a formal limit of integrals over piece-wise straight paths, taking the length of the straight pieces to zero in the limit. For more details, we point the reader to [3].

In the case of gravity we want to use an analogy between paths and space-times to construct an expression that can lead us to a theory of Quantum Gravity. Imagine some spatial slice $\mathcal{S}_i$ of a space-time geometry at some time 0, and some other spatial slice $\mathcal{S}_f$ at some time T. We wish to calculate the transition amplitudes between these spaces by means of a propagator $G(\mathcal{S}_i, \mathcal{S}_f; T)$. In order to do this, we generalize (2) into an expression for this propagator. Let $\Gamma(\mathcal{S}_i, \mathcal{S}_f; T)$ be the set of all space-times $[g_{\mu\nu}]$ connecting $\mathcal{S}_i$ and $\mathcal{S}_f$ in time T, where $[g_{\mu\nu}]$ is defined as the class

of Lorentzian metrics on a manifold $\mathcal{M}$ equivalent to $g_{\mu\nu}$ under diffeomorphisms. Now we define

$$G(\mathcal{S}_i, \mathcal{S}_f; T) = \int_{[g_{\mu\nu}]\in\Gamma(\mathcal{S}_i,\mathcal{S}_f;T)} D[g_{\mu\nu}] \exp\left(iS([g_{\mu\nu}])\right). \tag{3}$$

This expression is known as the Gravitational Path Integral. We still have some choice in S, but we will only consider the action suggested by GR, namely the Einstein-Hilbert action

$$S([g_{\mu\nu}]) \propto \int_{\mathcal{M}} d^{n+1}x\sqrt{-g}\left(R - 2\Lambda\right), \tag{4}$$

with $\mathcal{M}$ then $n+1$ dimensional manifold on which $[g_{\mu\nu}]$ lives, g the (negative valued) determinant of the Lorentzian geometry $[g_{\mu\nu}]$, R the Ricci scalar curvature and Λ the cosmological constant. This is the action for pure gravity, meaning we consider a universe that does not contain any matter fields. Note that for $n = 1$ the integral of the Ricci scalar is a purely topological quantity by the Gauss-Bonnet theorem. Unfortunately for us, it is not a priori clear how one should calculate (3). Standard approaches of perturbative renormalisation that are often used to make sense of path integrals do not seem to work in the case of four dimensional gravity. We therefore need a nonperturbative approach to make sense of this expression and give it a workable definition.

2.1 Discretization of the Path Integral

One approach to nonperturbative QG is to define the integral over smooth curved space-time geometries as a limit of piecewise flat geometries (where the volume of a flat building blocks tends to 0 in the limit). One can see this as an analogy to how in the path integral of QM, the space of paths was constructed as the limit of spaces of piecewise straight paths. This has originally been studied in the context of Euclidean gravity and Dynamical Triangulations, where piecewise flat geometries are built from triangular (or more generally simplicial) building blocks (triangulations) [4, 5]. This line of study has not yet lead to a fruitful theory of Quantum Gravity in four dimensions, but it did inspire some new approaches, which form the starting point of this thesis.

The general idea of using triangulations to study the Gravitational Path Integral (3) is as follows. We consider a (finite set of) triangular (simplicial) $n+1$-dimensional building block(s) and impose a flat metric on them. This means that all metric properties of these building blocks are encoded in the lengths of its one-dimensional edges. Then we look at the set of all possible geometries obtained from gluing these building blocks together along matching n-dimensional faces (using some set of gluing rules) such that it connects two n-dimensional geometries $\mathcal{S}_i, \mathcal{S}_f$ constructed from the faces of the building blocks, separated by a time T (using some notion of time that we have defined on our geometries). This gives us a countable set of geometries $\Gamma(S_i, S_f, T)$, such that we can replace our integral by a sum.

$$G(\mathcal{S}_i, \mathcal{S}_f; T) = \sum_{\mathcal{T}\in\Gamma(\mathcal{S}_i,\mathcal{S}_f;T)} \frac{1}{C_{\mathcal{T}}} \exp\left(iS(\mathcal{T})\right). \tag{5}$$

Here $C_{\mathcal{T}}$ is the order of the automorphism group as a remnant of the measure on geometries after triangulation [4]. Note that for the Einstein-Hilbert action of a triangulation $\mathcal{T}$ one can calculate the integral over the curvature by adding up the deficit angles at all $n-1$-dimensional hinges of the simplicial building blocks, but when working with two-dimensional space-times, we are often not interested in this term due to the Gauss-Bonnet theorem, and we will just ignore it. Since from now on we will be only considering $n = 1$, or two-dimensional space-time, that means that

for a triangulation $\mathcal{T}$ from k different building blocks, where each building block j occurs $N_j(\mathcal{T})$ times, the Einstein-Hilbert action is given by

$$S(\mathcal{T}) = -\sum_{j=1}^{k} \lambda_j N_j(\mathcal{T}), \tag{6}$$

where λ_j is the product of the cosmological constant with the volume of building block j, which form the coupling constants of our theory. Typically it is possible to get rid of the factor i in the complex valued "path sum" (5), and map it injectively onto a real-valued expression with a form similar to a partition function. Such a real-valued expression is often easier to study. This transformation is the result of mapping Lorentzian geometries in the "path-sum" to Euclidean geometries by some form of analytic continuation, similar to a Wick-rotation. In the general, there is no prescription for mapping a given Lorentzian metric onto a Euclidean metric. However, for specific choices of flat building blocks, such a map can be defined, see for instance [6]. For our purposes, where we will only be considering two-dimensional models, it suffices to say we will be studying the expression

$$G(\mathcal{S}_i, \mathcal{S}_f; T) = \sum_{\mathcal{T} \in \Gamma(\mathcal{S}_i, \mathcal{S}_f; T)} \frac{1}{C_{\mathcal{T}}} \exp\left(-\sum_{j=1}^{k} \lambda_j N_j(\mathcal{T}) \right). \tag{7}$$

This leaves us with a choice for building blocks and gluing rules. Perhaps the most straightforward approach where one uses a single Euclidean building block, is that of the aforementioned Dynamical Triangulations. Since this approach was not very successful at describing a physical theory in four dimensions, other approaches with different building blocks and gluing rules have been proposed. More specifically, models have been proposed that implement a causal structure on the geometries by making a distinction between space-like and time-like edges of a (Lorentzian) building block and introducing appropriate gluing rules to enforce such a causal structure. Two of these models are, in the order of them being proposed, Causal Dynamical Triangulations (CDT) and Locally Causal Dynamical Triangulations (LCDT). In this thesis we aim to discuss an analytical study of the latter (in the two-dimensional case), but first we will define CDT and discuss the analytical solution of that, since we will use similar methods to study LCDT.

3 Two dimensional Causal Dynamical Triangulations

The model of Causal Dynamical Triangulations was first introduced in [7] as a two-dimensional model, where it was also solved analytically. Later it was generalized into higher dimensions [8], whereof no analytical solution is known. These higher dimensional models have been studied extensively using numerical simulations [9, 10]. For the purpose of this thesis we will only discuss the two dimensional case. We will also be discussing the analysis of the model and the extraction of a continuum limit. This will follow the same lines as [7] and for a more complete discussion on the matter we point the reader to this article. However, since most of the analysis done for this thesis has been largely based on the techniques used to study CDT, this has been added to this thesis for completeness.

There are various ways to define the class of CDT geometries. The building block of 2D CDT is a triangle with two time-like edges and one space-like edge (STT-triangles). The triangles are glued to each other along their time-like edges, to form a ring of triangles connecting two loops of space-like edges, as seen in figure 3. These rings can be stacked onto each other by gluing two space-like loops with the same number of edges onto each other. Each of these rings can be seen as a time-step, such that each space-like loop in the geometry can be labelled with a discrete time, starting with 0 at the bottom and going through the natural numbers until the top is reached. It is therefore said that CDT is characterised by a strict time foliation. Figure 4 shows a piece of CDT geometry where this foliation can be seen clearly. Alternatively, CDT geometries can be generated by gluing the STT-triangles together in such a way that at each internal vertex we have a local light cone structure, i.e. the edges from that vertex form four bundles, alternating space-like and time-like. Furthermore the geometry must have two boundary components, each forming a loop of space-like edges. Of course at this boundary one only has three bundles of edges connected to each vertex, two space-like and one time-like.

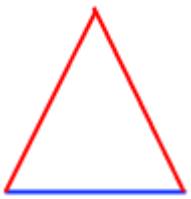

Figure 2: An STT triangle, blue stands for space-like, red for time-like

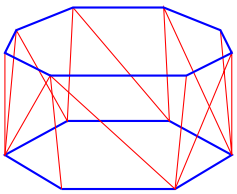

Figure 3: A ring of STT-triangles

The only intrinsic geometric aspect of a one-dimensional loop is its length. Given the fact that a space-like edge in CDT has a fixed length (say a), any spatial slice of CDT is characterised by the number of edges. Let $\Gamma_{\text{CDT}}(l_i, l_f; t)$ be the number of CDT geometries having one boundary with l_i edges labelled with time 0 and one boundary with l_f edges labelled with time t. We define the propagator for CDT as

$$G(l_i, l_f; t) = \sum_{\mathcal{T} \in \Gamma_{\text{CDT}}(l_i, l_f; t)} \frac{1}{C_{\mathcal{T}}} \exp\left(-\lambda N_{\mathcal{T}}\right), \tag{8}$$

with $N_{\mathcal{T}}$ the total number of triangles in the triangulation $\mathcal{T}$ and λ the coupling constant after analytical continuation of the expression onto a real valued expression.

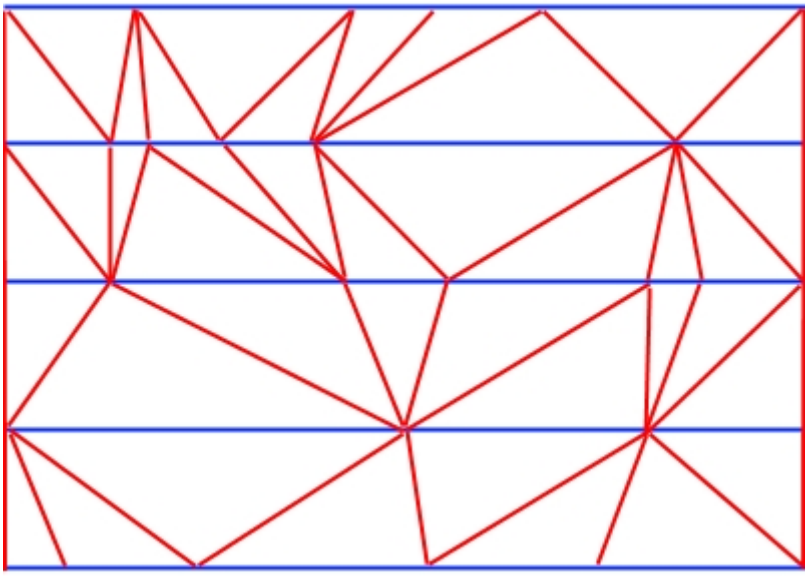

Figure 4: A piece of CDT geometry

3.1 Solving 2D CDT

In studying (8), it is actually easier to mark one of the vertices on the entrance loop (labelled time 0). Let $\Gamma^*_{\text{CDT}}(l_i, l_f; t)$ denote the triangulations with a marked vertex, then

$$G(l_i, l_f; t) = \frac{1}{l_i} \sum_{\mathcal{T} \in \Gamma^*_{\text{CDT}}(l_i, l_f; t)} \exp\left(-\lambda N_{\mathcal{T}}\right). \tag{9}$$

Note that by the fact that we can stack geometries, and all geometries are constructed by stacking rings, we have for any $t, t' > 0$

$$G(l_i, l_f; t) = \sum_{l=1}^{\infty} \frac{1}{l_i} \sum_{\mathcal{T} \in \Gamma^*_{\text{CDT}}(l_i, l; t)} \exp\left(-\lambda N_{\mathcal{T}}\right) \sum_{\mathcal{T}' \in \Gamma^*_{\text{CDT}}(l, l_f; t')} \exp\left(-\lambda N_{\mathcal{T}'}\right). \tag{10}$$

To exploit this fact, we define a generating function

$$\underline{G}(x, y; g; t) = \sum_{l_i=1}^{\infty} \sum_{l_f=1}^{\infty} x^{l_i} y^{l_f} \sum_{\mathcal{T} \in \Gamma^*_{\text{CDT}}(l_i, l_f; t)} g^{N_{\mathcal{T}}}, \tag{11}$$

such that

$$G(l_i, l_f; t) = \frac{1}{l_i} \left[\underline{G}(x, y; e^{-\lambda}; t)\right]_{x^{l_i} y^{l_f}}. \tag{12}$$

Equation (10) implies for any $t, t' > 0$

$$\underline{G}(x, y; g; t + t') = \oint \frac{dz}{2\pi i z} \underline{G}\left(x, \frac{1}{z}; g; t\right) \underline{G}(z, y; g; t'), \tag{13}$$

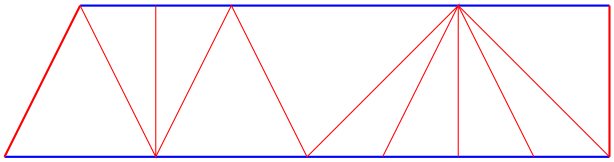

Figure 5: A ring cut into a strip

where the contour that we integrate over includes the singularities in z of $\underline{G}\left(x, \frac{1}{z}; g; t\right)$, but not those of $\underline{G}(z, y; g; t')$.

If we can find the generating function $\underline{G}(x, y; g; t = 1)$, we can use (13) to calculate an iteration equation for the generating function $\underline{G}(x, y; g; t)$. $\underline{G}(x, y; g; t = 1)$ keeps track of the number of single time-step rings that can be constructed in CDT, where one of the vertices on the entrance loop has been marked. Given such a ring, we can cut the ring into a strip by cutting along the rightmost time-like edge connected to the marked vertex. This means that the leftmost vertex on the bottom of this strip has only one time-like edge connected to it. Such a strip is illustrated in figure 5. Any of these strips can also be made into a ring by gluing the time-like boundaries together. This means that the generating function of the ring is the same as that of the strip (given the restriction on the leftmost bottom vertex). Also since each space-like loop in CDT consists at least of one edge, this must also be the case for the space-like boundaries of the strip. Let us first consider strips with no restrictions on vertices and with the possibility of space-like boundaries of length 0. Let $f(x, y, g)$ be the generating function of these unrestricted strips. Since each triangle has exactly one space-like edge, and every edge on the space-like boundary has to be part of a triangle, we have

$$f(x, y, g) = \sum_{n=0}^{\infty} \sum_{m=0}^{\infty} a_{n,m} (xg)^n (yg)^m, \tag{14}$$

where $a_{n,m}$stands for the number of strips with space-like boundaries of n and m edges. Given a strip with $n, m > 0$, we can remove the rightmost triangle, which either has its space-like edge at the top or bottom of the strip. This gives

$$a_{n,m} = a_{n-1,m} + a_{n,m-1} \tag{15}$$

This combined with the fact that $a_{n,0} = a_{0,m} = 1$ gives $a_{n,m} = \binom{n+m}{n}$. Therefore

$$f(x, y, g) = \sum_{n=0}^{\infty} \sum_{m=0}^{\infty} \binom{n+m}{n} (xg)^n (yg)^m = \frac{1}{1 - g(x + y)} \tag{16}$$

Since each of our restricted strips must have a left bottom vertex with only one time-like edge, the leftmost triangle must have its space-like edge at the bottom. We can therefore add this triangle to all unrestricted strips. Furthermore we should subtract all strips which have $m = 0$, which gives

$$\underline{G}(x, y; g; t = 1) = gx f(x, y, g) - \sum_{n=1}^{\infty} (gx)^n = \frac{g^2 xy}{(1 - gx)(1 - g(x + y))}. \tag{17}$$

We can now insert this into (13), which gives us

$$\underline{G}(x, y; g; t) = \frac{gx}{1 - gx} \underline{G}\left(\frac{g}{1 - gx}, y; g; t - 1\right). \tag{18}$$

This iteration equation will be the starting point for trying to extract a continuum theory out of CDT. Roughly speaking, we want to take the limit $a \to 0$ where a is our lattice spacing, the length of a single space-like edge. Naïvely, one would say that since we have absorbed the area of a single triangle into λ, we would have $\lambda \propto a^2$, but this will lead to uncontrolled divergences. In order to solve this problem, one has to renormalize the coupling constant and the propagator itself. We can interpret x, y as place-holders for boundary cosmological constant terms $x = \exp(-\lambda_i), y = \exp(-\lambda_f)$. Now the cosmological constants should undergo an additive renormalization. Using the canonical scaling ansatz, this gives for the boundary cosmological constants $\lambda_i = C_{\lambda_i} + Xa$, $\lambda_f = C_{\lambda_f} + Ya$ where X, Y have dimensions a^{-1}. Since $L_{i,f} = a l_{i,f}$, we get $x^{l_i} = x_c^{l_i} \exp(-XL_i)$ and $y^{l_f} = y_c^{l_f} \exp(-YL_f)$. For the cosmological constant λ the renormalization gives $\lambda = C_\lambda + \Lambda_R a^2$ or equivalently $g = g_c \exp(-\Lambda_R a^2)$ with Λ_R the renormalized cosmological constant with dimension a^{-2}. The propagator should undergo a multiplicative wave-function renormalization

$$\underline{G}_{\Lambda_R}(X, Y; T) = \lim_{a \to 0} a^\eta \underline{G}(x, y; g; t), \tag{19}$$

where we take $T = at$ since the geodesic height of each ring should scale with a. Now η and g_c should be chosen such that we get a non-trivial limit. This limit can be interpreted as some Laplace transform

$$\underline{G}_{\Lambda_R}(X, Y; T) = \int_0^\infty dL_i \int_0^\infty dL_f \, G^*_{\Lambda_R}(L_i, L_f; T) \exp(-XL_i) \exp(-YL_f). \tag{20}$$

Here $G^*_{\Lambda_R}(L_i, L_f; T)$ stands for the continuum propagator with a marked point on the entrance loop, which can be extracted by an inverse Laplace transform. This gives

$$G_{\Lambda_R}(L_i, L_f; T) = \frac{1}{L_i} G^*_{\Lambda_R}(L_i, L_f; T). \tag{21}$$

If we want to have

$$G_{\Lambda_R}(L_i, L_f; T + T') = \frac{1}{L_i} \int_0^\infty dL \, G^*_{\Lambda_R}(L_i, L; T) G^*_{\Lambda_R}(L, L_f; T) \tag{22}$$

as a continuum analogy of (10), such that we can interpret $G^*_{\Lambda_R}(L_i, L_f; T)$ as a transfer matrix, we can see from dimensional arguments that we must choose $\eta = 1$.

What remains is finding the correct g_c and taking the limit. Since in taking a limit we are only interested in leading order terms, we can set

$$x = x_c(1 - aX), \quad y = y_c(1 - aY), \quad g = g_c(1 - a^2 \Lambda_R). \tag{23}$$

If we want the limit to be non-trivial, i.e. finite and non-zero, we must find a triple x_c, y_c, g_c for which for all t $\underline{G}(x, y; g; t) = \mathcal{O}(a^{-1})$. It turns out that this holds for $x_c = y_c = 1$ and $g_c = \frac{1}{2}$. For $t = 1$ this can be checked explicitly, then from (18) we can work it out for all t. Due to the fact that $\frac{g}{1-gx} = x$ up to first order in a, we have $\underline{G}\left(\frac{g}{1-gx}, y; g; t-1\right) = \mathcal{O}(a^{-1})$ if $\underline{G}(x, y; g; t-1) = \mathcal{O}(a^{-1})$. Since $\frac{gx}{1-gx} = 1$ up to zeroth order in a, this also implies that $\underline{G}(x, y; g; t) = \mathcal{O}(a^{-1})$. Therefore this proves that $\underline{G}(x, y; g; t) = \mathcal{O}(a^{-1})$ for all t.

In order to find the continuum limit, we derive a differential equation for the continuum limit from (18). This can be done by subtracting a term $G(x, y; g; t-1)$ from the expression, which gives, up

to leading terms in a

$$\underline{G}(1-aX,1-aY;\frac{1}{2}(1-a^2\Lambda_R);t)-\underline{G}(1-aX,1-aY;\frac{1}{2}(1-a^2\Lambda_R);t-1)=$$
$$\underline{G}(1-a(X+a(2\Lambda_R-X^2)),1-aY,\frac{1}{2}(1-a^2\Lambda_R);t-1)-\underline{G}(1-aX,1-aY;\frac{1}{2}(1-a^2\Lambda_R);t-1)-$$
$$2Xa\underline{G}(1-aX,1-aY;\frac{1}{2}(1-a^2\Lambda_R);t-1). \quad (24)$$

Taking the limit $a \to 0$ gives

$$\frac{\partial}{\partial T}\underline{G}_\Lambda(X,Y;T)=\frac{\partial}{\partial X}(\Lambda-X^2)\underline{G}_\Lambda(X,Y;T), \quad (25)$$

where we have absorbed a factor 2 into the cosmological constant. This differential equation can be solved using standard techniques, as done in [7].

As an alternative to finding a differential equation for the continuum propagator, one could solve (18) directly and take a continuum limit of the closed form solution of the propagator generating function. This is only possible because (18) is of a form which allows for finding a closed form solution rather easily, but we will see later on that this is not always the case.

4 Two dimensional Locally Causal Dynamical Triangulations

In the previous section on CDT we have seen that causal structure can be implemented by forcing a strict time foliation on the triangulations. This condition also proved useful in solving the model analytically. However, strict time foliation is not a necessary condition for causal structure. One can therefore wonder whether the time foliation is an essential property of the discrete theory for arriving at the continuum theory that we have found in the previous section or not. Would it be possible to describe a discrete theory that implements a causal structure and does not make use of a time foliation, but would lead us to the same continuum limit, or would such a geometry lead us to a different limit. In order to study this, a variation on CDT without a global foliation has been proposed in [11]. This model is called Locally Causal Dynamical Triangulations (LCDT). Numerical simulations of this model in both two dimensions [12] and three dimensions [11], have suggested that the answer to this question depends on the dimension of our space-times. In the three-dimensional case, LCDT reproduced similar behaviour to CDT, while in two dimensions it was found that CDT and LCDT seem to have different properties that survive in the continuum limit. Therefore we are interested in an exact computation of the continuum limit for 2D CDT , which would allow for a rigorous comparison of CDT and LCDT.

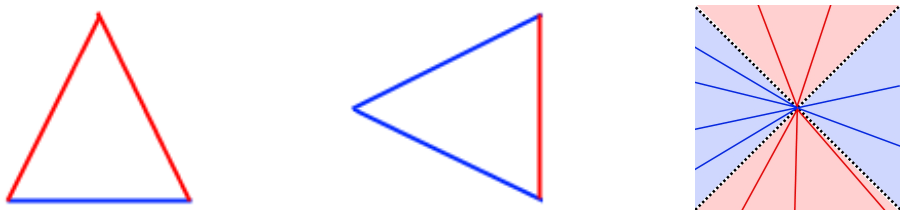

(a) An STT-triangle (b) An SST-triangle (c) A local light-cone structure

Figure 6: The building blocks and gluing rules of a 2D LCDT geometry

As mentioned before, it is possible to define CDT geometries by a local condition on the gluing of triangles around vertices to form a "light-cone" (local causal structure or vertex causality). Due to choice of the STT building block in CDT this resulted in the foliation (global causal structure) [13]. It turns out that if we also allow for a second triangular building block with two space-like edges and one time-like edge (SST-triangle) vertex causality does not imply the global causal structure. We get geometries with a well-behaved causal structure around each vertex, but no ensured foliation. We therefore define two-dimensional LCDT by the set of triangulations constructed from the SST and STT building blocks using the vertex causality condition. In figure 7 a piece of a generic LCDT geometry is illustrated. One can show that, under suitable conditions, nice properties of CDT such as invariance of topology in the spatial slices of the geometries and the absence of future-directed time-like paths starting and ending at the same space-like boundary component are also implied in LCDT geometries [14].

While in CDT, the notion of time on a geometry was quite clear, given by the number of rings separating the entrance and exit loop. Even though the actual physical interpretation of this notion of time is not entirely understood, from a combinatorial point of view it is a very useful definition. In LCDT the right choice of time is not as apparent as in CDT. In this thesis we will use various different notions of time, depending on what is convenient for the situation we are considering.

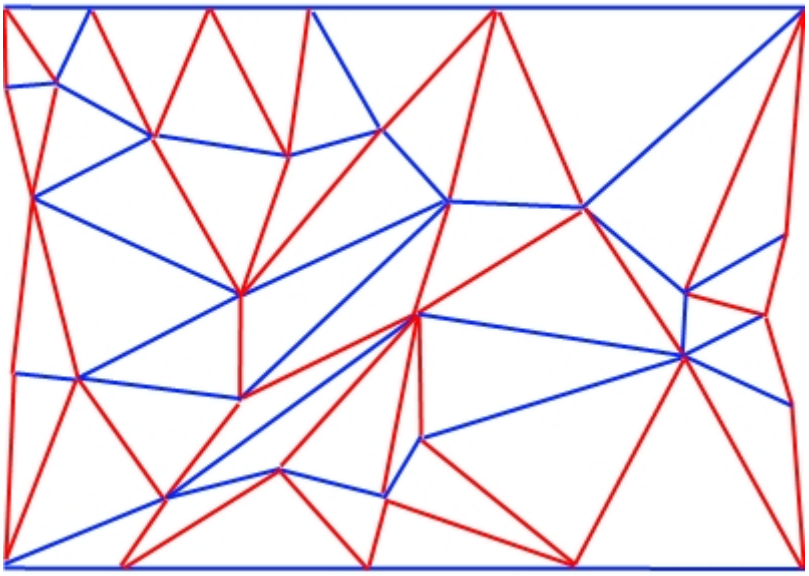

Figure 7: A piece of LCDT geometry

Suppose we have defined notion of time t, we want to calculate a propagator between space-like geometries, just as we did for CDT. Calling $\Gamma_{\text{LCDT}}(l_i, l_f; t)$ the set of LCDT geometries that connect two space-like geometries of l_i and l_f edges separated by a time t, we get an expression of the form

$$G(l_i, l_f; t) = \sum_{\mathcal{T} \in \Gamma_{\text{LCDT}}(l_i, l_f; t)} \frac{1}{C_{\mathcal{T}}} \exp\left(-\lambda_1 N_{\text{STT}}(\mathcal{T}) - \lambda_2 N_{\text{SST}}(\mathcal{T})\right). \tag{26}$$

Here we have two coupling constants instead of one, λ_1 and λ_2, for each of the two types of building blocks, the STT and SST triangles. $N_i(\mathcal{T})$ gives the number of building blocks of type i in the geometry $\mathcal{T}$. Just as before, it is often more convenient to study the propagator generating function

$$\underline{G}(x, y; g_1, g_2; t) = \sum_{l_i=1}^{\infty} \sum_{l_f=1}^{\infty} x^{l_i} y^{l_f} \sum_{\mathcal{T} \in \Gamma^*_{\text{LCDT}}(l_i, l_f; t)} g_1^{N_{\text{STT}}(\mathcal{T})} g_2^{N_{\text{SST}}(\mathcal{T})}. \tag{27}$$

As will become apparent during this thesis, we were forced to make simplifying assumptions and add additional structure to $\Gamma^*_{\text{LCDT}}(l_i, l_f; t)$ in order to say anything meaningful about the model. We will be discussing three approaches by which we try to derive combinatorial results on LCDT geometries, or some more simplified subsets of these. In some special cases, we will also be able to say something about the continuum limit.

4.1 Bubble-time approach

As has been discussed before in [14], it may be useful to study LCDT geometries constructed from stacking bubbles (referring to it as bubble CDT). In this section we show that under certain boundary conditions any LCDT geometry can be constructed from stacking bubbles, as one also can construct CDT geometries from stacking ring geometries. This will lead us to a notion of time

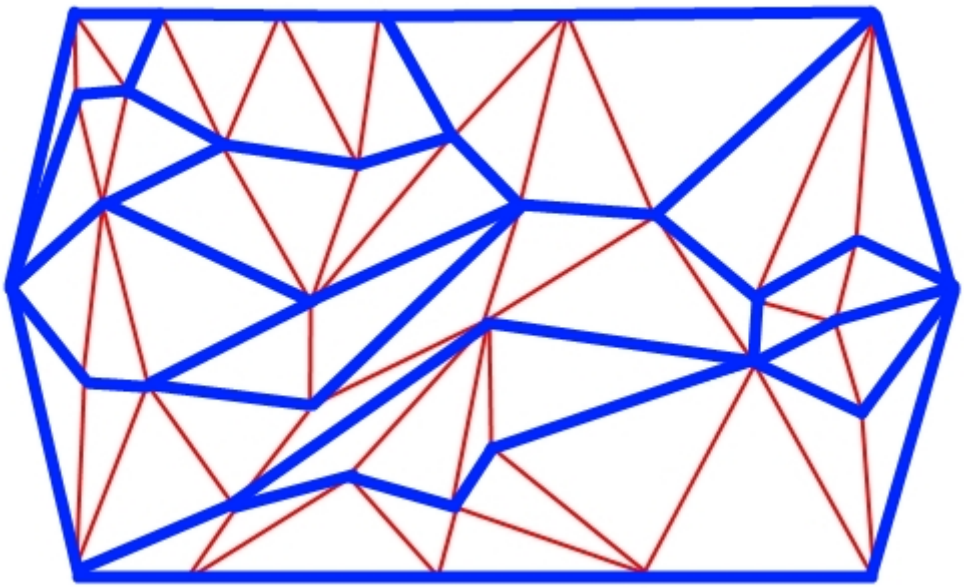

Figure 8: A pinched geometry consisting of bubbles

given by the number of bubbles in the LCDT geometry, analogous to how the number of rings in a CDT geometry defines the total time of the geometry. We will exploit this notion of time (where we do not claim that this time has any immediate physical interpretation) to derive an evolution equation for the LCDT propagator generating function. Unfortunately, at this point this evolution equation has not led us to a continuum theory.

We start by defining the geometries we will work with in this section. As noted in [14], periodic boundary conditions of space-like geometries for LCDT do not necessarily give bubble CDT geometries, but rather a class of geometries referred to as spiral CDT. In order to limit ourselves to the bubble CDT case, we will use open boundary conditions instead of periodic boundary conditions. This means that instead of considering space-like loops as initial and final geometry, we consider line segments, i.e. a sequence of space-like edges with free boundaries. For reasons that will become clear later, we allow these line segments to have length 0, only consisting of a single vertex. The triangulations that connect these geometries must consist of the LCDT building blocks and conform to its gluing rules, where we impose that the boundary edges that are not part of the initial and final space-like geometry to be time-like. Furthermore we allow for singularities, in the sense that just as the initial and final geometry can have length 0, we allow the two time-like boundary sections to share any number of vertices and edges. Finally we introduce two additional vertices for each time-like boundary section (which might only consist of a single vertex if the initial and final geometries touch at their ends) and connect all vertices on these boundaries to the corresponding additional vertex with space-like edges. For practical purposes, we label one of these vertices rightmost and the other leftmost. We will refer to these structures as pinched geometries. An example of such a pinched geometry is shown in figure 8.

Now we make the following claim: every one of these pinched geometries (as long as it has non-zero finite volume) can be constructed by stacking bubbles. Furthermore any stack of bubbles is a pinched geometry. Let us first describe what we mean by a stack of bubbles.

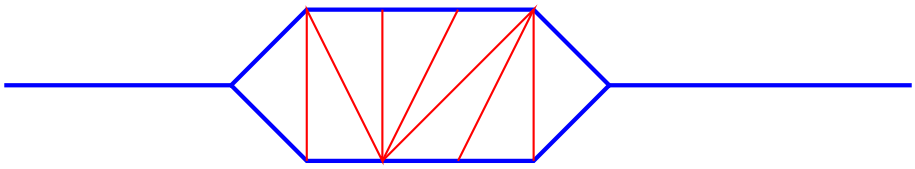

Figure 9: A single bubble geometry

We define a single bubble geometry by a pinched geometry as described above which includes exactly two SST-triangles. These single bubbles can be characterised in the following way: an unrestricted strip of STT-triangles in between the two SST-triangles. The additional left and right vertices are connected via a path of space-like edges to one of the SST-triangles. See figure 9 for an illustration.

If one glues two of these single bubbles together along space-like boundaries with matching length, one again obtains a pinched geometry. Furthermore, by repeating this process, we can obtain any pinched geometry.

We can prove this as follows. Given any pinched geometry (consisting of a non-zero number of triangles), by construction the two space-like boundaries have to coincide at both the left and right ends. Therefore, from the left and right, one can find at least two vertices where the boundaries diverge. At these vertices the only edges allowed to connect to this, are space-like. This means that only SST-triangles are situated at this vertex. We can thus conclude that the leftmost and rightmost triangles that share an edge with the bottom boundary are of the SST type, where the triangle at the left has its time-like edge at the right and at the right the time-like edge must be the left of the triangle. Now we can state that there is a leftmost SST-triangle with its time-like edge on the left at the bottom boundary. There also has to be an SST-triangle at the bottom boundary with the time-like edge to the right situated left of the aforementioned triangle. If there are multiples of these, select the rightmost of these. This means we have found two SST-triangles at the bottom boundary with time-like edges pointing towards each other, such that there are no other SST-triangles in between. All edges on the boundary in between these triangles have to be part of a triangle as well, otherwise they would be part of both bottom and top space-like boundaries, meaning there would need to be additional SST-triangles in between the pair we have selected. Thus all of these edges are part of an STT-triangle. Since the boundary of pinched geometries is completely space-like and due to local causal structure, there have to be other STT-triangles to complete the space in between the two SST-triangles into a strip. This means we have identified a single bubble, which we can remove from the geometry, leaving another pinched geometry behind. Since this entire process can be repeated, it shows that any pinched geometry is made up of single bubbles. Furthermore it is easy to see that each stack of bubbles results in a pinched geometry.

Now we identify the number of bubbles that make up a pinched geometry with a discrete "time" t. We would like to write an iterative equation for the propagator generating functions of these geometries for this time parameter, just as has been done for CDT when time was identified with the number of ring layers that made up the triangulations. Naïvely, this would give us a one-step

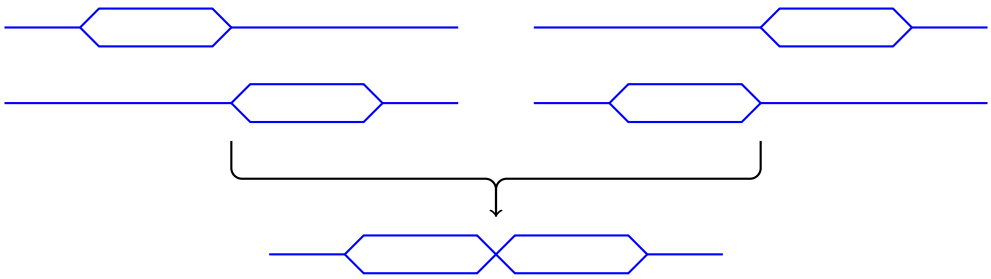

Figure 10: By purely stacking bubbles one over-counts the amount of geometries

propagator generating function

$$G(x,y;g_1,g_2;t=1) = g_2^2 \sum_{n_1,n_2,n_3,n_4=0}^{\infty} (xy)^{n_1+n_2} \binom{n_3+n_4}{n_3} (xg_1)^{n_3} (yg_1)^{n_4}$$
$$= \frac{g_2^2}{(1-xy)^2(1-g_1(x+y))}. \quad (28)$$

However, we have to take into account the following point. Unlike in CDT, changing the order in which you stack your time-steps (in this case the single bubbles) may result in constructing the same geometry. This is illustrated in figure 10. This means that if we would describe our geometries by a sequence of bubbles, we over-count. I our sum over geometries, each distinct geometry must be counted exactly once, no matter how they were constructed. In order to avert over-counting, we choose to always stack bubbles from left to right whenever there is an ambivalence (i.e. when multiple bubbles are located next to each other, and could therefore be stacked in any order, without making a difference). To keep track of this, we introduce variables that give the starting position of a bubble (the position of the SST-triangle closest to the leftmost vertex) and make sure that the next bubble we place is not fully to the left of this position. We do this as follows: Given a single bubble geometry, we mark two edges on the boundary, one we label s_i and the other s_f, where s_f is the upper edge of the first SST-triangle from the left and s_i can be any edge on the lower boundary that precedes the edge of the rightmost SST-triangle or is this edge itself if it is not the rightmost edge of the geometry. The reason for doing this is that by matching up not only the lengths of consecutive bubbles but also the marking s_i of a bubble with the s_f of a preceding bubble, this ensures that we stack bubbles from left to right, therefore making this bubble stacking procedure a unique way to generate our pinched geometries. This is illustrated in figure 11.

Note that if we mark edges on the boundary of a general pinched geometry, where s_i is associated with the leftmost bubble on the bottom and s_f with the rightmost bubble on the top, this defines a propagator $G(l_i,l_f;s_i,s_f;t)$ for triangulations $\Gamma(l_i,l_f;s_i,s_f;t)$ with bottom length l_i, top length l_f and edge labels s_i and s_f consisting of t bubbles that satisfies

$$G(l_i,l_f;s_i,s_f;t+t') = \sum_{l=0}^{\infty}\sum_{s=0}^{l} G(l_i,l;s_i,s;t)G(l,l_f;s,s_f;t'). \quad (29)$$

Now we can define the propagator generating function

$$\underline{G}(x,y;\alpha,\beta;g_1,g_2;t) = \sum_{l_i,l_f,s_i,s_f} x^{l_i}y^{l_f}\alpha^{s_i}\beta^{s_f} \sum_{\mathcal{T}\in\Gamma(l_i,l_f;s_i,s_f;t)} g_1^{N_{STT}(\mathcal{T})}g_2^{N_{SST}(\mathcal{T})}. \quad (30)$$

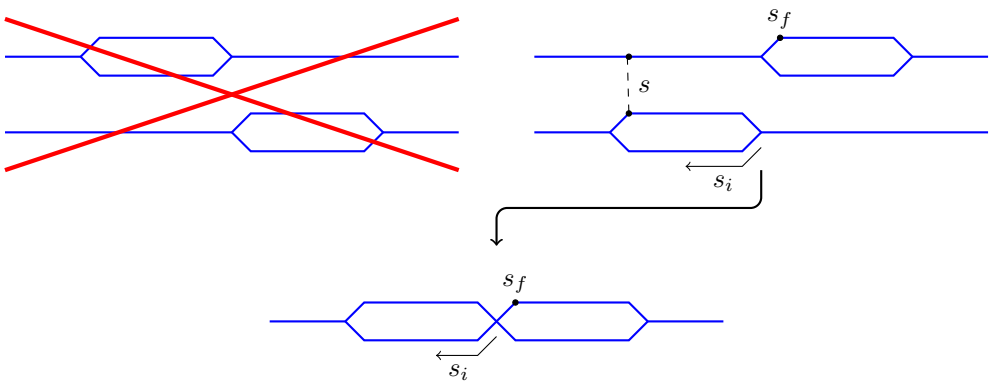

Figure 11: By introducing extra markings we can overcome the problem of over-counting

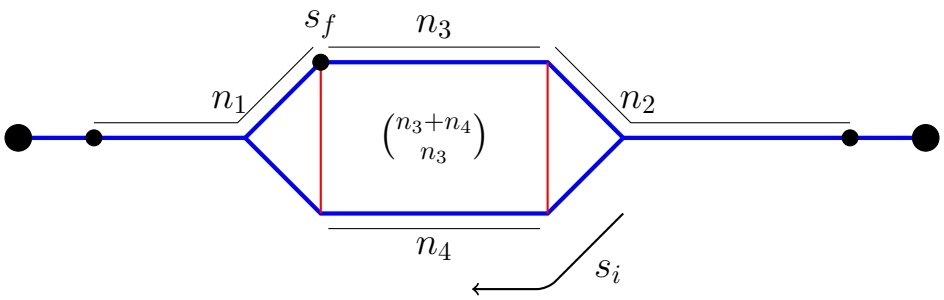

Figure 12: Parameters for constructing a propagator generating function for a single bubble geometry

Due to (29) this function satisfies

$$\underline{G}(x,y;\alpha,\beta;g_1,g_2;t+t') = \oint \frac{dz}{2\pi i z} \oint \frac{d\omega}{2\pi i \omega} \underline{G}(x,1/z;\alpha,1/\omega;g_1,g_2;t)\underline{G}(z,y;\omega,\beta;g_1,g_2;t'). \quad (31)$$

Just as in how CDT was solved, we construct the generating function for a $t = 1$ geometry (i.e. a single bubble geometry). It is useful to distinguish between the lengths of various boundary sections (as illustrated in figure 12) and then sum over all of these possible lengths. This gives

$$\begin{aligned}
&\underline{G}(x,y;\alpha,\beta;g_1,g_2;t=1) \\
&\quad = g_2^2 \sum_{n_1,n_2,n_3,n_4=0}^{\infty} (xy\beta)^{n_1}(xy)^{n_2}\binom{n_3+n_4}{n_3}(xg_1)^{n_3}(yg_1)^{n_4}\left(\sum_{n_5=0}^{n_1+n_3}\alpha^{n_5} + xy\alpha^{n_1+n_3+1}\right) \\
&= \frac{g_2^2}{(1-xy)(1-(y+\alpha x)g_1)}\left[\frac{\alpha xy}{1-\alpha\beta xy} + \frac{1}{(1-\alpha\beta xy)(1-\beta xy)} + \frac{g_1 x}{(1-\beta xy)(1-(x+y)g_1}\right],
\end{aligned} \quad (32)$$

Then we use (31) to derive an iteration equation for the propagator generating function for arbitrary

t

$$\underline{G}(x,y;\alpha,\beta;g_1,g_2;t+1) = g_2^2\left[\frac{\alpha^2\underline{G}(x,y;\alpha,\beta;g_1,g_2;t)}{(1-\alpha)(\alpha g_1 x^2+g_1-x)}+\right.$$
$$\left(\frac{\alpha g_1}{(\alpha-1)(\alpha g_1 x^2+g_1-x)}-1\right)\frac{\alpha\underline{G}(\frac{g_1}{1-x\alpha g_1},y;\frac{x\alpha-(x\alpha)^2 g_1}{g_1},\beta;g_1,g_2;t)}{1-x\alpha g_1}+$$
$$\left.\frac{x\underline{G}(x,y;1,\beta;g_1,g_2;t)}{(1-\alpha)(x-g_1-g_1x^2)}+\frac{g_1\underline{G}(\frac{g_1}{1-xg_1},y;\frac{x-x^2g_1}{g_1},\beta;g_1,g_2;t)}{(1-\alpha)(1-g_1x)(g_1x^2+g_1-x)}\right]. \quad (33)$$

When comparing this equation to (18), it is rather more complicated. First of all we have quite a higher number of terms than in the CDT case, in other words, the function $G(.,.;.,.;.,.;t)$ occurs multiple times on the right hand side of the equation. This means that the chances of directly solving this equation will be slim. Unless terms start to cancel while iterating this equation, the typical length of the expression for $G(x,y;\alpha,\beta;g_1,g_2;t)$ will grow exponentially in t. Furthermore, if one wishes to take a direct continuum limit from this equation, the problem is that it is not obvious how to deal with α and β. These variables have no physical meaning as far as we are aware, they were introduced just as a bookkeeping device. In fact, in the end we are only interested in the function $G(x,y;0,1;g_1,g_2;t)$, since the specifics of where bubbles start and end at the boundary are of no interest to us, once we have found all geometries. However, as is apparent from (33), in order to work out $G(x,y;0,1;g_1,g_2;t)$, one needs to know $G(x,y;\alpha,1;g_1,g_2;t)$ for different values of α as well. (This is of course not surprising, if this wasn't the case, the introduction of α and β wouldn't have been necessary.) This makes taking a continuum limit especially difficult, since in CDT the continuum limit was given by the behaviour of the function $G(x,y;g;t)$ near critical values of $x,y=1$, $g=\frac{1}{2}$. In this case, if we were to assert that the critical values here are, among others, also $x,y=1$, $g_1=\frac{1}{2}$, we would have to investigate the behaviour of the function $G(x,y;\alpha,\beta;g_1,g_2;t)$ around both $\alpha=0$ and $\alpha=1$. At this point we have not yet been able to find an appropriate way to study the continuum limit from (33), if there is any. Nevertheless we have shown it is possible to write down an iteration equation for (slightly modified) LCDT geometries. Perhaps it is therefore possible to find simpler iteration equations for more simplified versions of LCDT geometries, with notions of time that suit these simplifications. This is what we will be investigating in the rest of the thesis.

4.2 Graph-geometry approach

As our previous attempt to solve the LCDT model (using some specific choice of boundary conditions) has not led us to a continuum limit, we will now try to simplify the model by adding additional structure. We will do this by constructing the geometries we will work with from specific types of graph drawings, which will in a sense span the geometry. While it is certainly not true that this construction allows us to take into account all geometries that are of an LCDT type, we hope that it allows us to use a large enough ensemble of geometries to account for the features of an LCDT model.

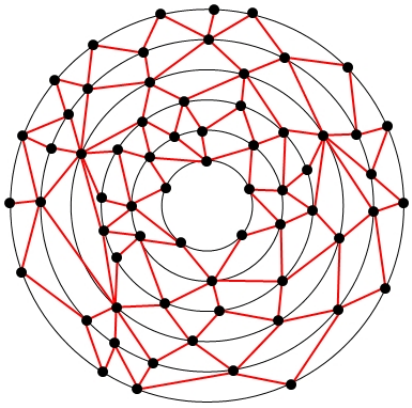

Figure 13: A graph drawing of time-like edges of some CDT geometry, the black rings show vertices of equal time, where the flow of time is from the center to the outer ring. Note that the space-like edges are not part of the digraph drawing, but can be added in a unique way.

Using graphs to span geometries is an idea that has also been used in studying CDT [15]. The time-like lines of a CDT geometry form a connected planar digraph drawing, such that the drawing forms a ring. The direction is given by the "flow of time". Furthermore we can assign a time t to each vertex, starting at the sources, labelled $t = 0$. Once one has labelled a vertex t, one then labels each vertex connected to it via an outgoing edge $t + 1$. A necessary feature of these CDT time-like graphs is that this prescription is not ambiguous, i.e. each path following the flow of time that connects one of the sources to a vertex must have the same length (number of edges), reflecting the time foliation of the CDT model. This length also defines the time of that vertex. Lastly, the fact that CDT geometries are built from STT-triangles is reflected by subgraphs given by the vertices labelled t and $t + 1$ and the edges connecting forming a (weakly) connected digraph ring for any t (as long as there are any vertices labelled $t+1$ in the digraph to begin with). The total time is given by the maximum t over all vertices. One can reconstruct the CDT geometry from these graphs by adding the space-like links to complete all the triangles.

We would like to generalize these graphs to a set of digraphs on which we can define a mapping to a large class of LCDT geometries. The term large is not defined here, rather as we will see the image of this mapping contains geometries of both the CDT type and geometries that are not identifiable with CDT, but solely with LCDT. To do this we will drop the features of the graph reflecting the foliation and the STT building blocks.

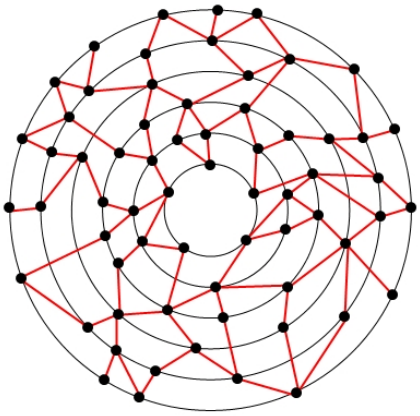

Figure 14: A graph drawing of time-like edges spanning some LCDT geometry. Once again, the black rings show vertices of equal time and the flow of time is from the center to the outer ring.

Once again we consider a planar digraph (not necessarily connected). Each vertex has been assigned an integer time t such that each vertex with time t can only be connected via an outgoing edge to a vertex of time $t' > t$. If there exists a vertex with time t and another with time t', then for any integer t'' such that $t < t'' < t'$, there must be a vertex with time t''. Once again the total time is defined by the maximum t over all vertices. As a simplifying assumption, we impose that if a vertex with time t is connected to a vertex with time $t' > t$, then all outgoing edges must connect to a vertex with time t'. Lastly, we impose that it should be possible to connect each of the sources to one additional vertex. This should also hold for the sinks. Note that these graphs cannot be completed to an LCDT geometry in a unique way by adding space-like edges. In order to find a unique prescription of completing graphs into triangulations, we choose to not only add space-like edges, but also additional time-like edges. We do this in the following way: Once again we can recognise bubbles in our geometry, however now in the time-like graph. A bubble is defined by two directed paths in the geometry which start at the same vertex and end at the same vertex (this may include the additional vertices at the bottom or top of the graph) such that in the space enclosed by these paths there are no additional vertices or edges. Note that this last statement depends on the way the time-like graph has been drawn, therefore it is important to stress that we construct our geometry not from the graph, but from the graph drawing. Two graph drawings are equivalent (and will give the same triangulations) if they can be continuously transformed into one another whilst remaining of the type we have defined. In such a graph drawing, each of the empty spaces is enclosed by such a bubble, i.e. two paths with coinciding starting and end points. We now add a vertex in the centre of each of these empty spaces and connect it to the starting and end points via time-like edges. Furthermore we connect each of the other vertices on the paths to the central vertex via space-like edges. Lastly, we remove the additional vertices at the top and bottom and all edges connected to it.

Note that this construction is injective. If we were given a triangulation that was constructed from a graph, we could regain the graph by removing all vertices and its connected edges that were placed in the center of bubbles. We can identify these vertices by how they connect via time-like lines to surrounding vertices. They connect to bubble sources and sinks, which (uniquely) have an odd number higher than 1 of time-like (outgoing or ingoing respectively) edges connected to them. This means we can identify bubble sources and sinks, which allows us to identify the bubbles and the vertices that were put in the center of those.

Now consider a digraph as described above with N_e edges, N_v vertices, n_i sources and n_f sinks. In the construction of a triangulation using these graphs, each triangle will have one edge that was part of the graph. Conversely, each edge in the graph will be a shared edge of two triangles in the triangulation. Therefore the total number of triangles will be $N_T = 2N_e$. Furthermore, the number of N_{STT} triangles can be calculated from the number of bubbles, since each bubble is filled by 4 STT triangles and some number of SST triangles. Note that on the boundary we can have half bubbles, i.e. bubbles of which the source or sink was one of the additional top or bottom vertices. If we count these bubbles as $\frac{1}{2}$, then this still gives the right number of N_{STT} triangles. In order to count the number of bubbles, we count the number of bubble sources (the number of vertices with an out-degree>1 times their out-degree-1) plus bubble sinks (the same as with sources, but with in-degree rather than out-degree). The number of bubbles is then this number divided by two. Therefore we have the following formula

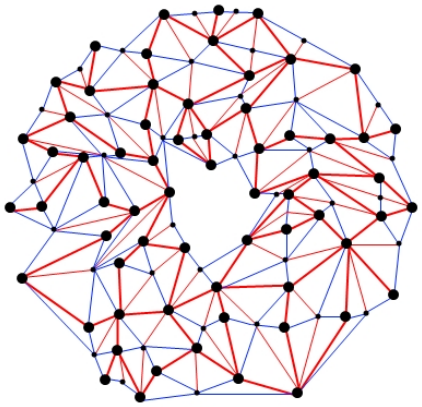

Figure 15: The LCDT geometry given by the graph drawing 14. The inner boundary is the entrance loop while the outer boundary is the exit loop.

$$\begin{aligned} N_{STT} &= 2\left(\sum_{v\in V}\max(0,\mathrm{indeg}(v)-1)+\max(0,\mathrm{outdeg}(v)-1)\right) \\ &= 2\left(\sum_{v\in V}(\mathrm{indeg}(v)+\mathrm{outdeg}(v)-2)+n_i+n_f\right) \\ &= 2\left(\sum_{v\in V}(\deg(v)-2)+n_i+n_f\right) \\ &= 2\left(2N_e-2N_v+n_i+n_f\right) = 4(N_e-N_v)+2(n_i+n_f). \end{aligned} \tag{34}$$

This means

$$N_{SST} = N_T - N_{STT} = 2N_e - 4(N_e - N_v) - 2(n_i + n_f) = 4N_v - 2(N_e + n_i + n_f) \tag{35}$$

Lastly, for the length of the space-like boundaries we have $l_i = 2n_i$, $l_f = 2n_f$.

Now let $N(N_e, N_v - n_f, n_i, n_f; t)$ be the number of our digraphs with N_e edges, N_v vertices, n_i sources, n_f sinks and a total time t. (The reason we chose $N_v - n_f$ to be one of the parameters is because it makes writing down an iteration equation for these numbers easier.) Just as in the CDT case, we work with geometries where one of the sources has been marked. The nice property of these numbers is that we can stack them, just as we did for CDT rings, by matching up sources

with sinks. This gives

$$N(N_e, N_v - n_f, n_i, n_f; t + t') = \sum_{n=1}^{\infty} \sum_{N'_e=0}^{N_e} \sum_{N'_v - n=0}^{N_v - n_f} N(N'_e, N'_v - n, n_i, n; t') N(N_e - N'_e, N_v - n_f + n - N'_v, n, n_f; t). \quad (36)$$

Using these numbers, we can now write down a propagator for our ensemble of geometries

$$G(l_i, l_f; t) = \frac{1}{l_i} \chi_{2\mathbb{N}}(l_i) \chi_{2\mathbb{N}}(l_f) \sum_{N_e, N_v} N(N_e, N_v - l_f/2, l_i/2, l_f/2; t) g_1^{4(N_e - N_v) + 2(n_i + n_f)} g_2^{4N_v - 2(N_e + n_i + n_f)}. \quad (37)$$

If we move to generating functions, where we let $N(\alpha, \beta, \gamma, \delta; t)$ be the generating function of $N(N_e, N_v - n_f, n_i, n_f, t)$,

$$N(\alpha, \beta, \gamma, \delta; t) = \sum_{i=0}^{\infty} \sum_{j=1}^{\infty} \sum_{k=1}^{\infty} \sum_{l=1}^{\infty} \alpha^i \beta^j \gamma^k \delta^l N(i, j, k, l). \quad (38)$$

Due to (36), we can once again make use of a contour integral

$$\underline{N}(\alpha, \beta, \gamma, \delta; t + t') = \oint \frac{dz}{2\pi i z} N\left(\alpha, \beta, \gamma, \frac{1}{z}; t\right) N(\alpha, \beta, z\delta; t'). \quad (39)$$

From (37), it follows that

$$\underline{G}(x, y; g_1, g_2; t) = \underline{N}\left(\frac{g_1^4}{g_2^2}, \frac{g_2^4}{g_1^4}, x^2 \frac{g_1^2}{g_2^2}, y^2 \frac{g_2^2}{g_1^2}; t\right). \quad (40)$$

Therefore, finding an iteration equation for N will result in an iteration equation for G. Note that this procedure of constructing geometries always results in an even number of triangles and initial and final edges. We therefore elect to count triangles and edges in pairs, since it will simplify the equations quite a bit. In taking the continuum limit, we then define our lattice spacing as the length of two edges, as we will see later on. Thus we define a generating function G_2 which counts the number of paired boundary edges instead of the number of edges in a triangulation, doing the same for the triangles, as the analytical continuation of

$$\underline{G}_2(x, y; g_1, g_2; t) = \underline{G}(\sqrt{x}, \sqrt{y}; \sqrt{g_1}, \sqrt{g_2}; t) \quad (41)$$

from the intersection of the area of convergence and the positive real numbers to the whole area of convergence. This means

$$\underline{G}_2(x, y; g_1, g_2; t) = \underline{N}\left(\frac{g_1^2}{g_2}, \frac{g_2^2}{g_1^2}, x\frac{g_1}{g_2}, y\frac{g_2}{g_1}; t\right). \quad (42)$$

Given one of our digraph drawings with total time t_{tot}, n_i sources and n_f sinks, with one marked source, we "cut" the graph along the rightmost path from this vertex, similarly to how one cuts a CDT cylinder into a strip. This gives us a strip-like graph, with two identical time-like boundaries, where the left boundary only has vertices with an out-degree ≤ 1 and on the top and bottom boundaries $n_i + 1$ and $n_f + 1$ points respectively. We wish to construct a "one-step function" for

these geometries. Any of the source vertices can either be part of a block of connected vertices within that single time step, or be a vertex that is disconnected. The contribution to the one-step function of a connected block can be derived in the same way as the unrestricted strip (16), yielding

$$\underline{N}_{\text{connected}}(\alpha,\beta,\gamma,\delta)=\sum_{n_i=1}^{\infty}\sum_{n_f=1}^{\infty}\binom{n_i+n_f-2}{n_i-1}(\beta\gamma)^{n_i}\delta^{n_f}\alpha^{n_i+n_f-1}=\frac{\alpha\beta\gamma\delta}{1-\alpha(\beta\gamma+\delta)}. \tag{43}$$

Furthermore, any single disconnected vertex has a contribution $\gamma\delta$, which means that any sequence of disconnected vertices have a contribution

$$\underline{N}_{\text{disconnected}}(\alpha,\beta,\gamma,\delta)=\sum_{n=0}^{\infty}(\gamma\delta)^n=\frac{1}{1-\gamma\delta}. \tag{44}$$

Note that we allow disconnected sequences of 0 vertices, so one can say that in between two connected blocks, we always have one disconnected sequence. This we use to write down a one-step function, where we note that each time step should at least have one connected block. We have to distinguish between different cases of how the two ends of the cut geometry are connected in the original geometry. Either the source vertex at which we cut is disconnected from the rest, it is part of a connected block that extends to the right of this vertex, or it is part of a connected block, but only with vertices to the left of it. This gives

$$\begin{aligned}\underline{N}(\alpha,\beta,\gamma,\delta;t=1)=&\sum_{n=1}^{\infty}\left(\frac{1}{1-\gamma\delta}\frac{\alpha\beta\gamma\delta}{1-\alpha(\beta\gamma+\delta)}\right)^n\frac{\gamma\delta}{1-\gamma\delta}+\\&\frac{1-\gamma\delta}{\delta}\sum_{n=1}^{\infty}\left(\frac{1}{1-\gamma\delta}\frac{\alpha\beta\gamma\delta}{1-\alpha(\beta\gamma+\delta)}\right)^n+\sum_{n=1}^{\infty}\left(\frac{1}{1-\gamma\delta}\frac{\alpha\beta\gamma\delta}{1-\alpha(\beta\gamma+\delta)}\right)^n\\&=\left(\frac{1}{1-\gamma\delta}+\frac{1-\gamma\delta}{\delta}\right)\frac{\alpha\beta\gamma\delta}{(1-\alpha\beta\gamma)(1-z_+\delta)(1-z_-\delta)}.\end{aligned} \tag{45}$$

Where we have

$$z_\pm=\frac{1}{2}\left(\gamma+\alpha\frac{\beta\gamma+1}{1-\alpha\beta\gamma}\pm\sqrt{\left(\gamma-\alpha\frac{\beta\gamma+1}{1-\alpha\beta\gamma}\right)^2+4\frac{\alpha\beta\gamma^2}{1-\alpha\beta\gamma}}\right). \tag{46}$$

Again one can use this one-step function to find a difference equation for the general function N in t using the same contour integral method as before, which gives

$$\begin{aligned}\underline{N}(\alpha,\beta,\gamma,\delta;t)=&\frac{\alpha\beta\gamma}{1-\alpha\beta\gamma}\left[\frac{\gamma\underline{N}(\alpha,\beta,\gamma,\delta;t-1)}{(\gamma-z_+)(\gamma-z_-)}+\right.\\&\left.\left((z_+-\gamma)+\frac{z_+}{z_+-\gamma}\right)\frac{\underline{N}(\alpha,\beta,z_+,\delta;t-1)}{z_+-z_-}+\left((z_--\gamma)+\frac{z_-}{z_--\gamma}\right)\frac{\underline{N}(\alpha,\beta,z_-,\delta;t-1)}{z_--z_+}\right].\end{aligned} \tag{47}$$

Since $\underline{N}$ and $\underline{G}_2$ are related via (42), we can write down

$$\begin{aligned}\underline{G}_2(x,y;g_1,g_2;t)=&\frac{g_1x}{1-g_1x}\left[\frac{g_2}{g_1}\frac{x\underline{G}_2(x,y;g_1,g_2;t-1)}{(x-z_+)(x-z_-)}+\right.\\&\left.\left((z_+-x)+\frac{g_2}{g_1}\frac{z_+}{z_+-x}\right)\frac{\underline{G}_2(z_+,y;g_1,g_2;t-1)}{z_+-z_-}-\left((z_--x)+\frac{g_2}{g_1}\frac{z_-}{z_--x}\right)\frac{\underline{G}_2(z_-,y;g_1,g_2;t-1)}{z_+-z_-}\right],\end{aligned} \tag{48}$$

with

$$z_{\pm} = \frac{1}{2}\left(x + \frac{g_2 x + g_1}{1 - g_1 x} \pm \sqrt{\left(x - \frac{g_2 x + g_1}{1 - g_1 x} \right)^2 + 4 \frac{g_2 x^2}{1 - g_1 x}} \right). \tag{49}$$

Note that in the limit $g_2 = 0$, we recover the CDT iteration equation

$$\underline{G}_2(x, y; g_1, 0; t) = \frac{g_1 x}{1 - g_1 x} \underline{G}_2 \left(\frac{g_1}{1 - g_1 x}, y; g_1, 0; t - 1 \right). \tag{50}$$

We would very much like to perform a continuum limit on (48), however at this point it is not obvious to us how to do this. Therefore we consider this work in progress. Of course in the $g_2 = 0$ limit, we do know how to take a continuum limit. But perhaps there are other simplifications we could make that also allow for a continuum limit, yet are still a non-trivial extension of the CDT model.

We introduce a further simplified graph model in which we do not allow for any connections between two vertices that have a time separation larger than one. Furthermore we do not allow a single vertex to be both sink and source, so any vertex must be connected to another vertex (given we have a geometry with a total time greater than zero). This means we reintroduce some foliation into the graph, so we have introduced a background foliation into the geometries that we consider. Even though the class of geometries is still larger than in the CDT case, this mildly foliated model might still resemble CDT too much to be of interest to us.

Just as above, we first derive an iteration equation for the generating function of our simplified graph drawings, $\underline{\tilde{N}}(\alpha, \beta, \gamma, \delta; t)$. From this we get an iteration equation for the generating function of our simplified LCDT geometries $\underline{\tilde{G}}_2(x, y; g_1, g_2; t)$. We start by calculating $\underline{\tilde{N}}(\alpha, \beta, \gamma, \delta; t = 1)$. We note that since each vertex at time t must always be connected to vertices at time $t+1$, unless $t = t_{\text{tot}}$, so each vertex in a single time step is part of a connected block. This gives

$$\underline{\tilde{N}}(\alpha, \beta, \gamma, \delta; t = 1) = \left(1 + \frac{1}{\delta} \right) \sum_{n=1}^{\infty} \left(\frac{\alpha\beta\gamma\delta}{1 - \alpha(\beta\gamma + \delta)} \right) = \frac{\alpha\beta\gamma}{1 - \alpha\beta\gamma} \frac{1 + \delta}{1 - \frac{\alpha + \alpha\beta\gamma}{1 - \alpha\beta\gamma}\delta}. \tag{51}$$

From this we can derive

$$\underline{\tilde{N}}(\alpha, \beta, \gamma, \delta; t) = \frac{\beta\gamma}{1 - \alpha\beta\gamma} \frac{1 + \alpha}{1 + \beta\gamma} \underline{\tilde{N}} \left(\alpha, \beta, \frac{\alpha + \alpha\beta\gamma}{1 - \alpha\beta\gamma}, \delta; t - 1 \right). \tag{52}$$

This results in the iteration equation

$$\underline{\tilde{G}}_2(x, y; g_1, g_2; t) = \frac{(g_2 + g_1^2)x}{(1 - g_1 x)(g_1 + g_2 x)} \underline{\tilde{G}}_2 \left(\frac{g_1 + g_2 x}{1 - g_1 x}, y; g_1, g_2; t - 1 \right). \tag{53}$$

This equation is very similar in form to (18), hinting this simplified graph model might be too similar to CDT. However, this does mean that we might be able to extract a continuum limit. To do this, we perform an additive renormalization on the coupling constants in the same way we did for CDT, which results in

$$g_1 \to g_1(1 - a^2\Lambda_1), \qquad g_2 \to g_2(1 - a^2\Lambda_2), \qquad x \to 1 - aX, \qquad y \to 1 - aY. \tag{54}$$

We define the continuum limit in the same way as before by a multiplicative wave function renormalization

$$\underline{\tilde{G}}_{\Lambda_1, \Lambda_2}(X, Y, T) := \lim_{a \to 0} a \underline{\tilde{G}}_2(1 - aX, 1 - aY; g_1(1 - a^2\Lambda_1), g_2(1 - a^2\Lambda_2); t). \tag{55}$$

For small a, (53) gives

$$\begin{aligned}
&\underline{\tilde{G}}_2(1-aX,1-aY;g_1(1-a^2\Lambda_1),g_2(1-a^2\Lambda_2);t)\\
&=\frac{g_1^2+g_2}{(1-g_1)(g_1+g_2)}\left(1-\left(\frac{g_1}{1-g_1}+\frac{g_1}{g_1+g_2}\right)aX+\mathcal{O}(a^2)\right)\underline{\tilde{G}}_2\left(\frac{g_1+g_2}{1-g_1}\left(1-\left(\frac{g_2}{g_1+g_2}+\frac{g_1}{1-g_1}\right)aX+\right.\right.\\
&\left.\left.a^2\left(\left(\frac{g_1g_2}{(g_1+g_2)(1-g_1)}+\frac{g_1^2}{(1-g_1)^2}\right)X^2-\left(\frac{g_1}{1-g_1}+\frac{g_1}{g_1+g_2}\right)\Lambda_1-\frac{g_2}{g_1+g_2}\Lambda_2\right)\right)+\mathcal{O}(a^3),y;g_1,g_2;t-1\right).
\end{aligned}\tag{56}$$

As we wish to extract a differential equation for $G_\Lambda(X,Y,T)$, we can impose a condition on the critical values g_1 and g_2, such that the continuum limit can be derived from the behaviour of $\tilde{G}_2$ around a single critical point. These conditions are

$$\frac{g_1+g_2}{1-g_1}=1\implies\frac{g_1^2+g_2}{(1-g_1)(g_1+g_2)}=1.\tag{57}$$

This gives us a free parameter $g\in\left[0,\frac{1}{2}\right]$ such that $g_1=g$ and $g_2=1-2g$. Inserting this into (56) gives

$$\begin{aligned}
&\underline{\tilde{G}}_2(1-aX,1-aY;g(1-a^2\Lambda_1),(1-2g)(1-a^2\Lambda_2);t)\\
&\qquad=\left(1+\frac{2g}{1-g}aX+\mathcal{O}(a^2)\right)\times\\
&\underline{\tilde{G}}_2\left(1-a\left(X+a\left(\frac{2g\Lambda_1+(1-2g)\Lambda_2}{1-g}-\frac{g}{1-g}X^2+\mathcal{O}(a^2)\right)\right),y;g_1,g_2;t-1\right).
\end{aligned}\tag{58}$$

Now we define the renormalized cosmological constant

$$\Lambda:=\frac{2g\Lambda_1+(1-2g)\Lambda_2}{g}.\tag{59}$$

This results in a differential equation similar to (25).

$$\left[\frac{\partial}{\partial T}+\frac{g}{1-g}\frac{\partial}{\partial X}(X^2-\Lambda)\right]\underline{\tilde{G}}_\Lambda(X,Y,T)=0\tag{60}$$

From this we can conclude that

$$\underline{\tilde{G}}_\Lambda(X,Y,T)=\underline{G}_\Lambda^{CDT}\left(X,Y,\frac{g}{1-g}T\right),\tag{61}$$

where $\underline{G}_\Lambda^{CDT}(X,Y,T)$ is the solution to (25) (given initial conditions). We can therefore interpret our continuum limit as the CDT limit with a rescaled time parameter. Note that for $g=\frac{1}{2}$, we reproduce the CDT result, as expected, since this sets $g_2=0$, while for $g=0$, we have a static model, i.e. no evolution in time.

4.3 Local spatial symmetry approach

A feature of the triangulations in the simplified graph-geometry approach is that in each vertex, the same number of space-like edges are connected to the right and left of this vertex. As a simplification to the full class of geometries, we shall now consider only geometries with this local reflection symmetry.

Consider the set of cylindrical triangulations with a space-like entrance and exit loop, that has the symmetry of space-like edges at each vertex as discussed above. As always, before we can start thinking about what the propagator for this class of geometries would be, we need to define a notion of time on our geometries. We could once again choose for some sort of bubble-time, as we did in our first approach, but the reason we made this choice was out of convenience for the combinatorics, rather than that it has a physical interpretation. In CDT time can be defined by the length of time-like paths along the edges of triangles connecting the two loops. Here this length is independent of which path one selects. Even though this time-like length is not precisely the same as the continuum proper time, it does relate to a notion of time-like distance. Therefore we would also like to define our time by the length of some path. One could try to define time by an average path length, but this is not convenient for the combinatorics. As an attempt to find a balance between combinatorics and physical interpretation, we define time by the length of some path that we choose.

Mark a point on the initial loop of a triangulation, cut along the rightmost time-like path from this vertex to the final loop. We define the time of this geometry as the length of this particular path. Now let n be the number of space-like edges connected to the leftmost (and by our symmetry condition also the rightmost) vertex on the initial boundary of the strip geometry cut from the cylindrical geometry. Let $\underline{G}(x, y; g_1, g_2; t, n)$ be the propagator generating function of the geometries with time t and n space-like edges to each side of the marked vertex.

If $n > 1$, the geometry will have a sequence of bubbles at the lower space-like boundary. By removing this sequence of bubbles all at once, we end up with a triangulation with $n-1$ space-like edges to each side of the marked vertex, as illustrated in figure 16. We can use this to find a relation for $\underline{G}(x, y; g_1, g_2; t, n)$.

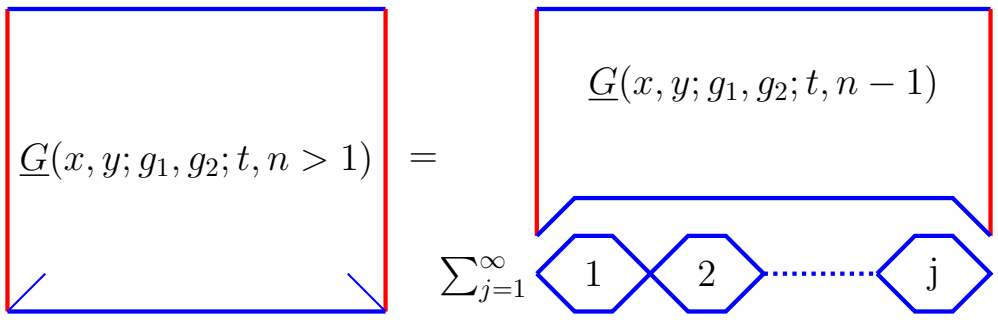

Figure 16: The removal of a sequence of bubbles from the bottom of a geometry while time t is unchanged

Once again we want to write down an iteration equation for the generating function using a contour

integral

$$\underline{G}(x,y;g_1,g_2;t,n) = \oint \frac{dz}{2\pi i z} f_1\left(x,\frac{1}{z};g_1,g_2\right)\underline{G}(z,y;g_1,g_2;t,n-1), \tag{62}$$

where f_1 encodes all possible sequences of bubbles.

$f_1(x,y;g_1,g_2) = \sum_{j=1}^{\infty}$ 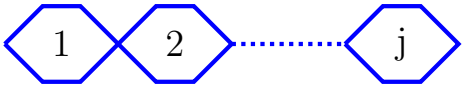

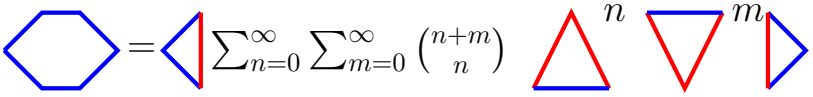

$$f_1(x,y;g_1,g_2) = \sum_{j=1}^{\infty}\left(\frac{(g_2xy)^2}{1-g_1(x+y)}\right)^j = \frac{(g_2xy)^2}{1-g_1(x+y)-(g_2xy)^2}. \tag{63}$$

Inserting this into (62) gives

$$\begin{aligned}\underline{G}(x,y;g_1,g_2;t,n) &= \oint \frac{dz}{2\pi i z}\frac{(g_2x)^2}{(1-g_1x)z^2-g_1z-(g_2x)^2}\underline{G}(z,y;g_1,g_2;t,n-1)\\ &= \frac{(g_2x)^2}{1-g_1x}\left[\frac{\underline{G}(z_+,y;g_1,g_2;t,n-1)}{z_+(z_+-z_-)}+\frac{\underline{G}(z_-,y;g_1,g_2;t,n-1)}{z_-(z_--z_+)}\right],\end{aligned} \tag{64}$$

where

$$z_\pm = \frac{g_1 \pm \sqrt{g_1^2+4(1-g_1x)(g_2x)^2}}{2(1-g_1x)}. \tag{65}$$

The generating function of the triangulations without restrictions on n is given by summing over n, which gives

$$\begin{aligned}\underline{G}(x,y;g_1,g_2;t) &= \sum_{n=1}^{\infty}\underline{G}(x,y;g_1,g_2;t,n)\\ &= \underline{G}(x,y;g_1,g_2;t,1)+\frac{(g_2x)^2}{1-g_1x}\left[\frac{\underline{G}(z_+,y;g_1,g_2;t)}{z_+(z_+-z_-)}+\frac{\underline{G}(z_-,y;g_1,g_2;t)}{z_-(z_--z_+)}\right].\end{aligned} \tag{66}$$

For $\underline{G}(x,y;g_1,g_2;t,n=1)$, we note that we can still remove a sequence of bubbles from the lower boundary, whilst respecting the boundary conditions (i.e. time-like boundaries on the sides of the sequence with only one time-like edge connected to the leftmost lower vertex). This is illustrated in figure 17.

Using f_2 to encode the removed bubble sequence, we have

$$\underline{G}(x,y;g_1,g_2;t,1) = \oint \frac{dz}{2\pi i z} f_2\left(x,\frac{1}{z};g_1,g_2\right)\underline{G}(z,y;g_1,g_2;t-1), \tag{67}$$

where

$$\begin{aligned}f_2(x,y;g_1,g_2) &= \frac{g_1x+(g_2xy)^2}{1-g_1(x+y)}\sum_{n=0}^{\infty}\left(\frac{(g_2xy)^2}{1-g_1(x+y)}\right)^n-\frac{1}{1-g_1x}\\ &= \frac{g_1x+(g_2xy)^2}{1-g_1(x+y)-(g_2xy)^2}-\frac{1}{1-g_1x}.\end{aligned} \tag{68}$$

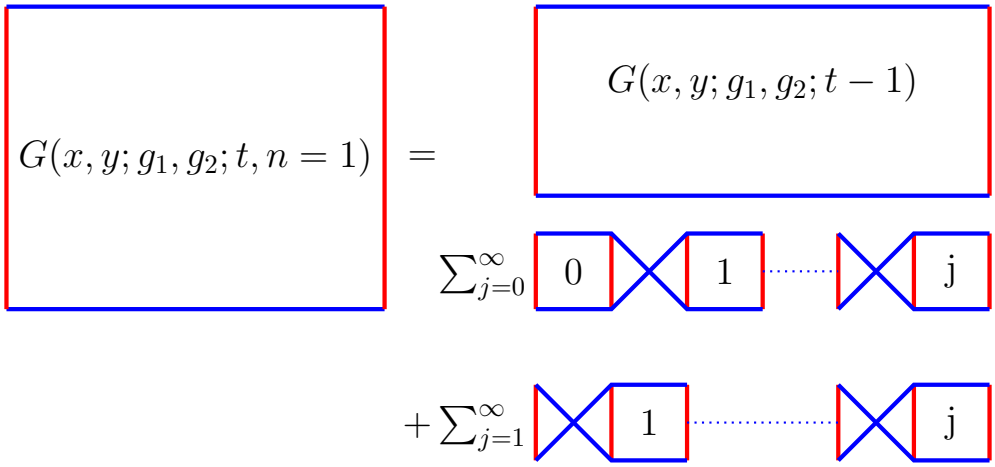

Figure 17: Removal of sequence of bubbles from bottom of the geometry such that time t decreases

This gives

$$\underline{G}(x,y;g_1,g_2;t,1) = \oint \frac{dz}{2\pi i}\frac{1}{1-g_1x}\frac{g_1xz+\frac{(g_2x)^2}{z}}{(z-z_+)(z-z_-)}\underline{G}(z,y;g_1,g_2;t-1)$$
$$= \frac{1}{1-g_1x}\left[\frac{\left(g_1xz_+ + \frac{(g_2x)^2}{z_+}\right)\underline{G}(z_+,y;g_1,g_2;t-1)}{z_+-z_-} + \frac{\left(g_1xz_- + \frac{(g_2x)^2}{z_-}\right)\underline{G}(z_-,y;g_1,g_2;t-1)}{z_--z_+}\right], \tag{69}$$

so

$$\underline{G}(x,y;g_1,g_2;t) = \frac{1}{1-g_1x}\left[\frac{\frac{(g_2x)^2}{z_+}\underline{G}(z_+,y;g_1,g_2;t) + \left(g_1xz_+ + \frac{(g_2x)^2}{z_+}\right)\underline{G}(z_+,y;g_1,g_2;t-1)}{z_+-z_-}\right.$$
$$\left. + \frac{\frac{(g_2x)^2}{z_-}\underline{G}(z_-,y;g_1,g_2;t) + \left(g_1xz_- + \frac{(g_2x)^2}{z_-}\right)\underline{G}(z_-,y;g_1,g_2;t-1)}{z_--z_+}\right]. \tag{70}$$

Note that once more this equation simplifies to (18) if we set $g_2 = 0$. By the radius of convergence of f_1 and f_2, we should renormalise such that

$$\lim_{a\to 0} 2g_1 + g_2^2 = 1. \tag{71}$$

So given some free parameter $g \in [0, \frac{1}{2}]$ we can define a continuum limit using

$$g_1 \to g(1-a^2\Lambda_1), \qquad g_2 \to \sqrt{1-2g}(1-a^2\Lambda_2), \qquad x \to 1-aX, \qquad y \to 1-aY. \tag{72}$$

This means $\lim_{a\to 0} z_- = -\frac{1-2g}{1-g}$, so $\lim_{a\to 0}\underline{G}(z_-,y;g_1,g_2;t) < \infty$. Furthermore $z_+ = 1-aX+\mathcal{O}(a^2)$. Since we use the initial condition $\underline{G}(x,y;g_1,g_2;t=0,n=1) = \frac{xy}{1-xy} = \mathcal{O}\left(\frac{1}{a}\right)$, it follows that we should define the continuum limit

$$\underline{G}_{\Lambda_1,\Lambda_2}(X,Y,T) = \lim_{a\to 0} a\underline{G}(1-aX,1-aY;g(1-a^2\Lambda_1),\sqrt{1-2g}(1-a^2\Lambda_2;t) \tag{73}$$

Using equation (70), we find

$$\lim_{a\to 0} a\underline{G}(1-aX,1-aY;g(1-a^2\Lambda_1),\sqrt{1-2g}(1-a^2\Lambda_2;t) = \\ \lim_{a\to 0} a\left(\frac{1-2g}{2-3g}+\mathcal{O}(a)\right)\underline{G}(1-aX+\mathcal{O}(a^2),1-aY;\sqrt{1-2g}(1-a^2\Lambda_1),g(1-a^2\Lambda_2;t)+ \\ a\left(\frac{1-g}{2-3g}+\mathcal{O}(a)\right)\underline{G}(1-aX+\mathcal{O}(a^2),1-aY;g(1-a^2\Lambda_1),\sqrt{1-2g}(1-a^2\Lambda_2;t-1)+\mathcal{O}(a). \tag{74}$$

Therefore

$$\lim_{a\to 0} a\underline{G}(1-aX,1-aY;g(1-a^2\Lambda_1),\sqrt{1-2g}(1-a^2\Lambda_2);t) = \\ \lim_{a\to 0} a\underline{G}(1-aX,1-aY;g(1-a^2\Lambda_1),\sqrt{1-2g}(1-a^2\Lambda_2);t-1), \tag{75}$$

meaning (70) is consistent with the continuum limit. Unfortunately, in order to derive a differential equation for $\underline{G}_{\Lambda_1,\Lambda_2}(X,Y,T)$, one has to take higher orders in a into account as well. This means that the terms $\underline{G}(z_-,y;g_1,g_2;t)$ also start to play a role. Therefore in order to derive the continuum limit, one would have to study the behaviour of $\underline{G}(x,y;g_1,g_2;t)$ both around $x=1$ and $x=-\frac{1-2g}{1-g}$. At this point we haven't found a way to do this, so we have not been able to derive a continuum limit yet.

Lastly, note that (70) is an implicit iteration equation, meaning it does not express $\underline{G}(x,y;g_1,g_2;t)$ purely as a function of $\underline{G}(x,y;g_1,g_2;t-1)$, but rather as a function of $\underline{G}(x,y;g_1,g_2;t)$ itself as well. If we had chosen a different notion of time, this equation could have been explicit. The notion of time that does this, is given by the number of bubble sequences that are stacked up on each other to form the geometry. Equivalently, one could define time by the number of space-like lines a time-like path from the entrance to the exit loop has to cross (where we consider a vertex with n space-like edges to the right and n to the left a point where n space-like lines are crossed). This is a time independent of the choice of path, but it does reintroduce some sense of foliation, as we can now label certain space-like loops uniquely with a discrete time parameter. Using the same arguments as above, one finds the iteration equation for this definition of time to be

$$\underline{G}(x,y;g_1,g_2;t) = \frac{1}{1-g_1x}\left[\frac{\left(g_1xz_+ + 2\frac{(g_2x)^2}{z_+}\right)\underline{G}(z_+,y;g_1,g_2;t-1)}{z_+-z_-}\right. \\ \left. + \frac{\left(g_1xz_- + 2\frac{(g_2x)^2}{z_-}\right)\underline{G}(z_-,y;g_1,g_2;t-1)}{z_--z_+}\right]. \tag{76}$$

The discussion of the continuum limit for this notion of discrete time remains roughly the same.

5 Conclusions

In this thesis we have discussed various ways to study two-dimensional LCDT geometries, with the specific goal to find a continuum limit of the LCDT model. We have tried various simplifications of the model, be it by choosing specific non-periodic boundary conditions, by adding some additional background structure or by imposing additional local structure. We have seen that these simplifications allow for deriving iteration equations for the generating functions associated with the discrete model. If one is only interested in the discrete model, these equations are essentially enough to calculate everything you want to know (as long as you can keep t bounded). After all, for arbitrary t one can just calculate the generating function by iterating these equations t times (at least in the cases where the iteration equation is explicit). Of course for large t it is quite a lot of work to calculate this, but it is possible, at least in principle. However, we are not primarily interested in the discrete model, but in the continuum limit that it may imply. So far we have only been able to find such a continuum limit in very selected cases, such as the original CDT model and the simplified graph model that we have introduced here. Unfortunately, for the more interesting cases that we discussed, namely those that take into account a considerably larger class of geometries than just the CDT geometries, we have so far not been able to find a proper continuum limit. Perhaps a closer analysis of the iteration equations will reveal a closed form solution for the discrete model, from which we can take the continuum limit directly. Unfortunately it is unknown to the author of this thesis how this could be done. Nevertheless I hope that with this thesis I have shed some new light on the LCDT model and I hope that it may lead others to new ideas for solving it.

6 Acknowledgements

This research was supported in part by Perimeter Institute for Theoretical Physics. Research at Perimeter Institute is supported by the Government of Canada through the Department of Innovation, Science and Economic Development and by the Province of Ontario through the Ministry of Research and Innovation. Furthermore I would like to thank the Radboud Honours Programme for their support and my supervisor, Professor Renate Loll for her advice and guidance throughout this project.

References

[1] S. W. Hawking. Particle creation by black holes. *Comm. Math. Phys.*, 43(3):199–220, 1975, http://projecteuclid.org/euclid.cmp/1103899181.

[2] C. Kiefer. Quantum gravity: general introduction and recent developments. *Annalen der Physik*, 15(1-2):129–148, 2006, arXiv:gr-qc/0508120.

[3] J. Zinn-Justin. *Path Integrals in Quantum Mechanics*. Oxford University Press, 2013.

[4] F. David. Simplicial quantum gravity and random latices. Lectures given at Les Houches école d'été de physique théorique, 1993, arXiv:hep-th/9303127.

[5] J. Ambjørn, B. Durhuus, and T. Jonsson. *Quantum Geometry, a statistical field theory approach*. Cambridge University Press, 1997.

[6] J. Ambjørn, A. Görlich, J. Jurkiewicz, and R. Loll. Nonperturbative quantum gravity. *Physics Reports*, 519(45):127 – 210, 2012, arXiv:1203.3591 [hep-th].

[7] J. Ambjørn and R. Loll. Non-perturbative lorentzian quantum gravity, causality and topology change. *Nuclear Physics B*, 536(1):407 – 434, 1998, arXiv:hep-th/9805108.

[8] J. Ambjørn, J. Jurkiewicz, and R. Loll. Nonperturbative lorentzian path integral for gravity. *Phys. Rev. Lett.*, 85:924–927, Jul 2000, arXiv:hep-th/0002050.

[9] J. Ambjørn, J. Jurkiewicz, and R. Loll. Emergence of a 4d world from causal quantum gravity. *Phys. Rev. Lett.*, 93:131301, Sep 2004, arXiv:hep-th/0404156.

[10] J. Ambjørn, A. Görlich, J. Jurkiewicz, and R. Loll. Planckian birth of a quantum de sitter universe. *Phys. Rev. Lett.*, 100:091304, Mar 2008, arXiv:0712.2485 [hep-th].

[11] S. Jordan and R. Loll. Causal dynamical triangulations without preferred foliation. *Physics Letters B*, 724(13):155 – 159, 2013, arXiv:1305.4582 [hep-th].

[12] R. Loll and B. Ruijl. Locally causal dynamical triangulations in two dimensions. *Phys. Rev. D*, 92:084002, Oct 2015, arXiv:1507.04566 [hep-th].

[13] D. Benedetti and J. Henson. Imposing causality on a matrix model. *Physics Letters B*, 678(2):222 – 226, 2009, arXiv:0812.4261 [hep-th].

[14] R. Hoekzema. Generalized causal dynamical triangulations in two dimensions, 2012, https://web.science.uu.nl/ITF/Teaching/2011/2012/Renee%20Hoekzema.pdf.

[15] B. Durhuus, T. Jonsson, and J. Wheater. On the spectral dimension of causal triangulations. *Journal of Statistical Physics*, 139(5):859–881, 2010, arXiv:0908.3643v2 [math-ph].